Quantum Dynamics of H_{2} Trapped within Organic Clathrate Cages

Timothy A. Strobel, Anibal J. Ramirez-Cuesta, Luke L. Daemen, Venkata S. Bhadram, Timothy A. Jenkins, Craig M. Brown, and Yongqiang Cheng

Phys. Rev. Lett. **120**, 120402 — Published 23 March 2018

DOI: 10.1103/PhysRevLett.120.120402

Quantum Dynamics of H_2 Trapped within Organic Clathrate Cages

Timothy A. Strobel,[1,*] Anibal J. Ramirez-Cuesta,[2] Luke L. Daemen,[2] Venkata S. Bhadram,[1] Timothy A. Jenkins,[3,‡] Craig M. Brown,[3] Yongqiang Chen[2]

[1] *Geophysical Laboratory, Carnegie Institution of Washington, Washington, D.C. 20015, USA*

[2] *Chemical and Engineering Materials Division (CEMD), Neutron Sciences Directorate, Oak Ridge National Laboratory, Oak Ridge, Tennessee 37831, USA*

[3] *Center for Neutron Research, National Institute of Standards and Technology, Gaithersburg, Maryland 20899, USA*

(Dated: March 14, 2018)

The rotational and translational dynamics of molecular hydrogen trapped within β-hydroquinone clathrate (H_2@β-HQ) — a practical example of a quantum particle trapped within an anisotropic confining potential—were investigated using inelastic neutron scattering (INS) and Raman spectroscopy. High-resolution vibrational spectra, including those collected from the VISION spectrometer at Oak Ridge National Laboratory, indicate relatively strong attractive interaction between guest and host with a strikingly large splitting of rotational energy levels compared with similar guest/host systems. Unlike related molecular systems in which confined H_2 exhibits nearly free rotation, the behavior of H_2@β-HQ is explained using a two-dimensional (2D) hindered rotor model with barrier height more than two times the rotational constant (-16.2 meV).

Particle in a box and the rigid rotor are fundamental physical concepts that represent simple, yet significant applications of the Schrödinger equation. For a diatomic molecule, translational energy levels can be modeled assuming a particle within a three-dimensional box, while rotational energy levels are given by $E(J) = BJ(J+1)$, where B is the rotational constant and J is the rotational quantum number. For the case of molecular hydrogen, the presence of two indistinguishable fermions requires that the overall wavefunction be antisymmetric and gives rise to two different nuclear spin isomers. H_2 molecules with antiparallel nuclear spins can only exist with even rotational states ($J = 0, 2, ...$, *para* H_2), while molecules with parallel nuclear spins must have odd rotational states ($J = 1, 3, ...$, *ortho* H_2). Quantum molecular dynamics are influenced by interaction potentials that may vary in spatial dimension, and practical examples of entrapped quantum particles within well-defined interaction potentials provide the rare opportunity to probe the coupled translational-rotational states under model-like conditions.

Clathrates are guest/host systems in which one set of molecular species encapsulates another [1]. Hydrogen trapped within cage-like guest/host materials has been of recent interest due to the ideal nature of these systems to understand quantum dynamics and for the possibility of these materials to store hydrogen for energy applications [2–11]. Clathrate cages provide ideal nanoscale confining potentials for small molecules, which can be probed by experiment and validated by rigorous quantum mechanical calculations. Water-based clathrate hydrates are the most notable class of these inclusion compounds, although others based on organic systems are known. Hydroquinone (Benzene-1,4-diol, HQ) is known to form clathrates (β-HQ) in the presence of small guest (G) molecules like methanol with the ideal composition 1G:3HQ [12]. Hydrogen is capable of stabilizing this clathrate phase at pressures up to ∼1.4 GPa, beyond which multiple H_2 molecules may occupy a single β-HQ cage (we will refer to the single occupancy H_2:3HQ form as H_2@β-HQ)[13, 14]. Guest/host interactions in H_2@β-HQ are substantial when compared with H_2 trapped in clathrate hydrate cages, [15, 16] and suggest fundamental differences in the quantum dynamics of the hydrogen molecule that can be probed by experiment. Here, we examine the translational and rotational dynamics of H_2 within β-HQ clathrate cavities using inelastic neutron and Raman scattering. In contrast with all previously reported molecular systems in which H_2 exhibits nearly free rotation, H_2 trapped within the cavities of β-HQ clathrate behaves as a two-dimensional (2D) hindered rotor with an impressively large splitting of rotational energy levels.

H_2@β-HQ was synthesized by pressurizing α-HQ with H_2 at ∼200 MPa, then samples were quenched to low temperature and the pressure was released. Inelastic neutron scattering (INS) and Raman measurements were performed at ambient pressure on samples kept at low temperature. Initial INS data were collected using the DCS Spectrometer (NIST Center for Neutron Research) and the TOSCA spectrometer (ISIS, Rutherford Appleton Laboratory), while the final high-resolution spectra were collected using the recently-constructed VISION spectrometer (Spallation Neutron Source, Oak Ridge National Laboratory). A complete record of the experimental details is provided in the supplemental information (SI).

INS spectra obtained from clathrates formed using *normal* hydrogen (n-H_2) represent a convolution of *ortho* and *para* hydrogen excitations, which complicates subsequent interpretation. Even at very low temperature, a mixture of spin isomers persists for long times due to the inefficiency of angular momentum exchange in the absence of a catalyst. We thus followed the method of Ulivi et al. [3] and performed two independent measurements using different *ortho*/*para* concentrations (one

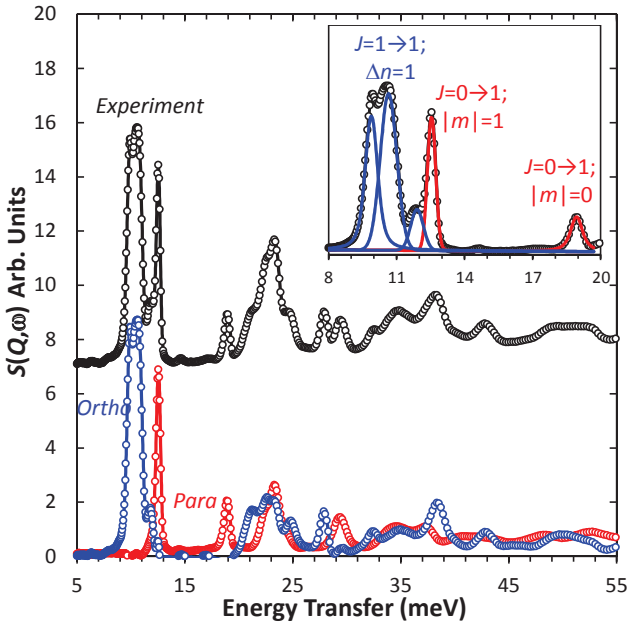

FIG. 1. Experimental INS spectra collected at VISION from sample formed using n-H_2 recorded at 5 K. Pure *ortho* and *para* contributions were obtained by measuring two different samples with known concentrations. The experimental spectrum is shifted upward from the individual *ortho* and *para* contributions. The inset shows the low-energy region with J=1 fundamental center-of-mass rattling modes and J=0 rotational doublet. Peaks were fit using Voigt profile functions.

formed from n-H_2, and another using nearly pure p-H_2) in order to extract the pure component spectra by linear combination (Fig.1) and make unambiguous assignments.

The J=1 spectrum consists of three resolvable features centered around 10.6 meV, which can be related to particle-in-a-box-type center of mass (c.o.m.) motion of H_2 within the clathrate cavities. This fundamental "rattling" transition is the principal excitation for o-H_2 (J=1→1). Following the nomenclature of Xu et al. [5], translational energy levels are described by three quantum numbers: the number of quanta, ν, the vibrational angular momentum along the z axis, $|l|$, and the translational z mode, ν_z. Excitations originating from changes in these energy levels are labeled Δn. Due to differences in scattering cross section (the p-H_2 translational cross section is only 2% of the ^{1}H incoherent cross section), the analogous transition for p-H_2 (J=0→0) has negligible intensity and is not considered. The three features at 9.9, 10.6 and 11.8 meV originate from anisotropy of the clathrate cages and are similar to H_2 within clathrate hydrates [3, 10] and anisotropic fullerides [7]. It is worth noting that the energies of the three resolvable J=1→1 features for H_2@β-HQ are nearly identical to H_2@$(H_2O)_{20}$, but are roughly half the energies for C_{60} and open-cage endofullerenes [7]. This fact likely reflects the larger size scale between the cages of clathrates and fullerene-based structures. For example, the translational energy levels for a particle in a sphere scale as $E \propto 1/mr^2$, where m is the mass of the particle and r is the radius of the sphere.

A sharp feature observed at 12.5 meV is clearly assigned as a rotational component in the J=0 spectrum. This assignment is supported by momentum transfer analysis and by a complimentary observation using the DCS spectrometer on the neutron energy gain side of the spectrum (see SI). This peak originates from the fundamental rotational transition of p-H_2 (J=0→1), which, for the case of freely-rotating solid H_2, occurs at 14.7 meV, *e.g.*, a rigid rotor with B = 7.35 meV. Other clathrates and fullerene-based materials show the principal transition centered near 14.7 meV, shifted and/or split by no more than ∼1.4 meV. In these cases, the rotational degeneracy is fully lifted and the three components of m, the quantum number representing the projection of angular momentum along z, for J=0→1 (i.e., m=-1,0,1) are observed, indicating mildly perturbed 3D rotation. No rotational triplet was observed here, unlike the case for water-based clathrates and anisotropic open-cage endofullerene [3, 7]. For H_2@β-HQ, a second sharp feature is observed at 18.9 meV and the integrated intensities between the 12.54 and 18.92 meV peaks occur in an approximate 2:1 ratio. The lack of a third rotational component points toward a 2D hindered rotor where the Hamiltonian can be modeled as

$$H = \frac{\hat{L}}{2I^2} + \frac{V_2}{2}(1 - cos2\theta) \ , \qquad (1)$$

where $\hat{L}$ is the angular momentum operator, I is the moment of inertia and V_2 describes the barrier height for a diatomic rigid rotor undergoing 2D rotation [17, 18]. In this case, θ is the polar angle between the molecular axis and the z axis. Treating the potential as a perturbation and expanding in spherical harmonics, we used the DAVE software [19] to calculate eigenvalues for 80 rotational levels with barrier heights between $0 \geq V_2 \geq -3B$ spread over 100 points on a uniform grid.

Using the approach above, the J=0→1 transition energy was reproduced with B=7.18 meV and V_2=-16.19 meV (-2.26B). The rotational constant, $B=\hbar^2/2\mu {r_e}^2$, is 95% of that for the free molecule, which implies an increase in the equilibrium separation, r_e, by ∼2.6%. Such an elongation would manifest itself as a significant redshift in the H_2 vibron frequency. Indeed, previous Raman measurements of the H_2 vibron show a softening of ∼50 cm^{-1} [13]. Fig.2 shows the pure o-H_2 and p-H_2 spectra with rotational transitions calculated from the 2D hindered rotor model. The 2D model explicitly predicts that the transition at 12.54 meV is doubly degenerate (m=±1) whereas the transition at 18.92 meV is a singlet (m=0). In addition to the rotational lines at 12.5 and 18.9 meV in the J=0 spectrum, two broader

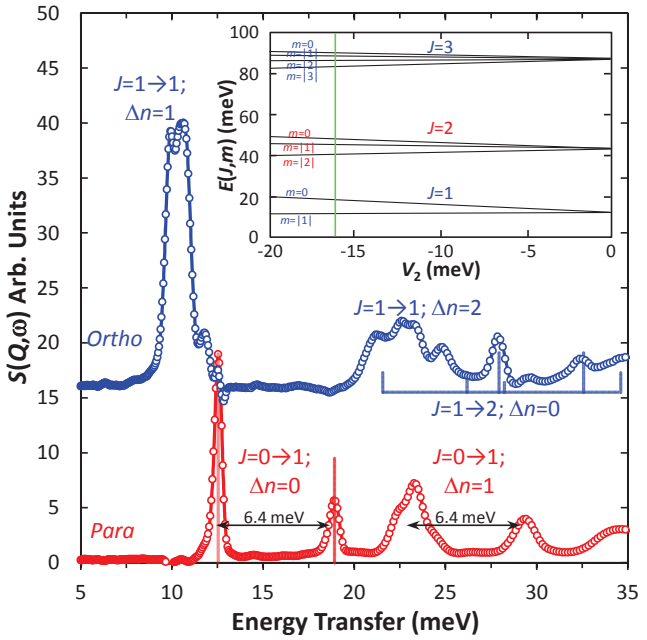

FIG. 2. INS spectra of pure *o*- and *p*-H_2 from VISION recorded at 5 K. Vertical bars indicate transition energies predicted by the 2D model. In the absence of rigorous intensity calculations, the relative heights of the vertical bars are simply scaled by the transition degeneracies. The inset shows calculated energies of the rotational transitions as a function of barrier height. The green vertical bar indicates a barrier energy of -2.26B.

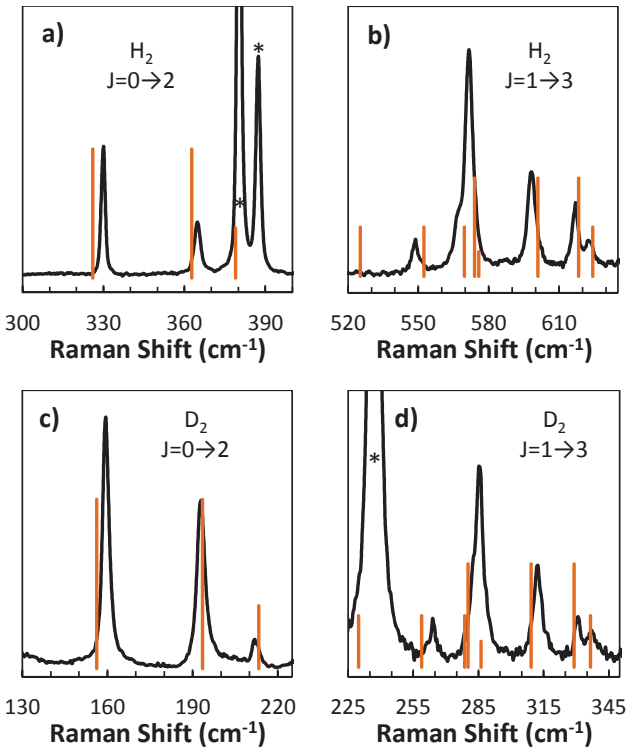

FIG. 3. Raman spectra for a-b) H_2@β-HQ and c-d) D_2@β-HQ clathrates at 77 K compared with calculated transition energies. Vertical bars indicate transition energies predicted by the 2D model where relative intensities are simply scaled by the transition degeneracies.

lines (apparently with multiple contributions) appear at 23 and 29.4 meV. Like the fundamental J=0→1 peaks, the higher-energy peaks are separated by ∼6 meV, but are shifted to higher energy by approximately 10.6 meV. Since 10.6 meV is the central position for the J=1→1 rattling modes, the bands centered near 23 and 29.4 meV are assigned to combined translation/rotational excitations, namely, J=0→1; Δn=1.

The hindered rotor model also predicts energies for the J=1→2 transitions, which should have measurable intensity. The model predicts six transitions with different energies, as shown by the vertical bars in Fig. 2. Several sharp features in the experimental J=1 spectrum show good correspondence with the predicted transition energies. For example, the sharp peak at 27.9 meV can be clearly assigned to J=1→2, with contributions from $|m|$=1→2 and $|m|$=0→0. In addition to the J=1→2 transitions, this energy range also has contributions from the first *o*-H_2 ratting overtone, J=1→1; Δn=2.

In order to further validate the 2D hindered rotor model, the calculated rotational transitions were compared with Raman data collected from a sample with a mixture of *o*- and *p*-H_2. In this case, sharp rotational transitions are observed at much higher energies than the INS data. Before making the comparison, we first review the Raman spectrum for the β-HQ clathrate host to make unambiguous assignments as several low-frequency host vibrations occur at similar energies to the H_2 rotational transitions. By comparing the Raman spectra from β-HQ clathrates formed with methanol and with H_2, the common host features were identified, allowing for accurate assignments of the H_2 roton modes (see SI). Like the vibron modes, the observed rotons for H_2@β-HQ are also significantly perturbed from their free-rotation values by up to ∼40 cm^{-1} [13].

Fig. 3 shows the J=0→2 and J=1→3 roton regions for H_2@β-HQ clathrate compared with calculated transition energies. Note that these regions are the only transitions accessible at the measurement temperature of 80 K. The intensities for the calculated transitions (represented by vertical bars) are approximated by the relative degeneracies associated with each transition. According to the 2D model, transition energies increase with decreasing $|m|$ for a given J. Fig. 3a shows the J=0→2 region for H_2. The model predicts three J=0→2 transitions ($|m|$=2, $|m|$=1, m=0) at 326 cm^{-1}, 363 cm^{-1} and 379 cm^{-1} with degeneracies of 2:2:1. The simple model captures the features of the experimental data remarkably well where two experimental transitions are located at 330 and 365 cm^{-1}, although a host lattice vibration masks the predicted highest-energy peak. For absolute

confirmation, we compare with the Raman spectrum of D_2@β-HQ clathrate. In this case the J=0→2 transitions are shifted to lower energy due to the higher mass and are not obscured by host lattice modes. For D_2, we have simply scaled B by the ratio of the reduced masses and assumed the same value for V_2 as for the H_2 case. For the case of D_2 (Fig. 3c) we clearly see the three components predicted for the J=0→2 transition, in semi-quantitative agreement with experiment: 156, 193 and 213 cm^{-1} for the model vs. 159 193 and 212 cm^{-1} for experiment. Remarkably, we also observe qualitative agreement between the model and experiment for the J=1→3 transitions for both H_2 and D_2 (Fig. 3b-d). Here, the situation is more complex as eight distinct transitions are possible from the two J=1 states (m=|1|, 0) to the four J=3 states (m=|3|, |2|, |1|, 0). Nevertheless, these features confirm the hindered 2D nature of H_2 trapped within β-HQ clathrate cavities.

While the translational behavior for H_2@β-HQ appears similar to previous observations in clathrate hydrates and fullerene-based systems and is easily related to particle-in-a-box-type motion, the fundamental nature of rotation appears quite different. For anisotropic fullerenes and water clathrates, the *para* hydrogen transition exists as a triplet that is centered near 14.7 meV and triplet splitting is on the order of ∼1 meV [3, 7]. This indicates only mildly perturbed 3D rotation as a consequence of potential anisotropy with respect to the orientation of the H_2 molecule. For the case of H_2@β-HQ clathrate we see different behavior in both the magnitude and nature of the interaction potential. In fact, the 2D hindered rotor model is most often used to describe H_2 adsorbed to metal surfaces [20–22] or binding sites such as those found in metal-organic framework compounds [23, 24]. The barrier height seems much greater than expected for a closed-shell molecular system with only weak, van der Waals type interactions, although rotational barrier and binding strength are not necessarily of a causal relation [25].

How is it that the cages of β-HQ clathrate mimic adsorption behavior of a 2D surface? The clathrate cavities are formed by two hexagonal $(OH)_6$ rings and six C_6H_6 groups. Three of the C_6H_6 groups point downward from the top $(OH)_6$ ring and three C_6H_6 groups point upward from the bottom $(OH)_6$ ring (Fig.4). Note that all host H atoms were replaced by D atoms for the INS experiment, but the behavior is independent of isotopic substitution as verified by the Raman measurements. This arrangement sets perfect conditions for anisotropy in terms of both chemical and spatial interactions. The $(OH)_6$ rings are stacked in layers along the z direction, separated by ∼5.4 Å, while the nearest-neighbor H and C atoms that form the equatorial cage walls are separated by ∼7 and 8 Å, respectively. This means that the cavity may be viewed approximately as an oblate spheroid where the semi-major axis is ∼1.5× the pole distance along the symmetry axis.

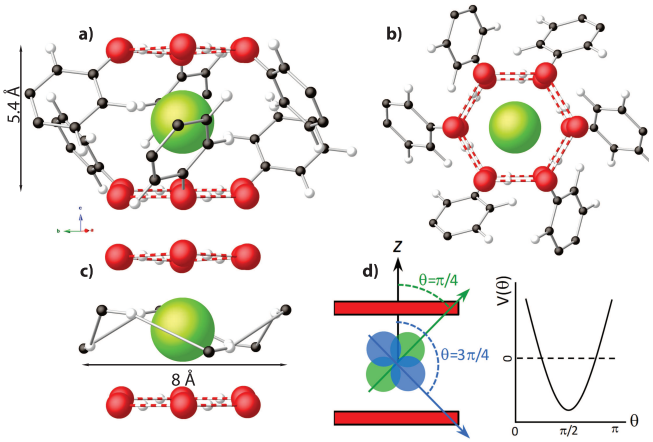

FIG. 4. β-HQ clathrate cavity viewed normal to a) (100) and b) (001). Portions of molecules surrounding the cage have been removed for clarity. Red, black, white and green spheres represent O, C, H (or D) and J=0 H_2, respectively. Striped bands connect O atoms to emphasize hydrogen-bonded hexagonal rings. c) Nearest-neighbor interactions between guest and host. Artificial bonds are drawn between some C and H atoms to emphasize the nearest equatorial interactions. d) Schematic of OH hexagonal rings acting as 2D confining surfaces and interaction potential as a function of polar angle.

The 2D rotor behavior is now apparent. The $(OH)_6$ rings can be effectively be thought of as confining surfaces. Given the short distance between the $(OH)_6$ rings compared with the equatorial C_6H_6 groups, the interaction potential is most favorable when the axis of the H_2 molecule lies parallel to the surface, and the potential remains attractive when the polar angle is between $\pi/4<\pi<3\pi/4$ with respect to the z direction (Fig. 4d)[26]. This configuration stabilizes the J=1; m=|1| rotational states that have "donut-shaped" probability density distributions, while the "p-orbital" shaped J=1; m=0 states have increased energy. The anisotropy of the potential is also confirmed by previous dielectric and quasi-elastic neutron measurements on H_2S@β-HQ clathrate where essentially free rotation was observed on the axis parallel to z, but significantly hindered rotation was observed in all other directions [27].

In summary, we report the first 2D hindered rotor behavior for H_2 trapped in a molecular clathrate, which provides a model-like practical system to probe the quantum molecular dynamics of confined hydrogen. The anisotropic confining potential produced by β-HQ clathrate cavities results in 2D hindered rotation with a barrier energy that is more than two times greater than the rotational constant. This observation strengthens the view that complex local interaction potentials, opposed to binding energies, are the primary driving force behind large shifts in rotational transition energies. We hope

that this study will motivate detailed quantum calculations of the coupled rotational-translational dynamics in related systems.

We thank J. Leao, M. Loguillo and M. Rucker for their help with experiments. This work was supported as part of the Energy Frontier Research in Extreme Environments (EFree) Center, an Energy Frontier Research Center funded by the U.S. Department of Energy, Office of Science under Award No. DE-SC0001057. This research benefited from use of the VISION beamline (IPTS-16698) at ONRL's Spallation Neutron Source which is supported by the Scientific User Facilities Division, Office of Basic Energy Sciences, U.S. Department of Energy, under Contract No. DE-AC0500OR22725 with UT Battelle, LLC. We gratefully acknowledge the Science and Technology Facilities Council (STFC) for access to neutron beamtime at ISIS, and also for the provision of sample preparation, TOSCA facilities.

* Corresponding author.
tstrobel@carnegiescience.edu

‡ Current address.
RDRL-WML-B, U.S. Army Research Laboratory, Aberdeen Proving Ground, Maryland 21005

[1] H. M. Powell, J. Chem. Soc. , 61 (1948).
[2] S. A. FitzGerald, T. Yildirim, L. J. Santodonato, D. A. Neumann, J. R. D. Copley, J. J. Rush, and F. Trouw, Phys. Rev. B **60**, 6439 (1999).
[3] L. Ulivi, M. Celli, A. Giannasi, A. J. Ramirez-Cuesta, D. J. Bull, and M. Zoppi, Phys. Rev. B **76**, 161401 (2007).
[4] K. T. Tait, F. Trouw, Y. Zhao, C. M. Brown, and R. T. Downs, J. Chem. Phys. **127**, 134505 (2007).
[5] M. Xu, F. Sebastianelli, and Z. Bačić, J. Chem. Phys. **128**, 244715 (2008).
[6] M. Xu, F. Sebastianelli, Z. Bačić, R. Lawler, and N. J. Turro, J. Chem. Phys. **129**, 064313 (2008).
[7] A. J. Horsewill, K. S. Panesar, S. Rols, M. R. Johnson, Y. Murata, K. Komatsu, S. Mamone, A. Danquigny, F. Cuda, S. Maltsev, M. C. Grossel, M. Carravetta, and M. H. Levitt, Phys. Rev. Lett. **102**, 013001 (2009).
[8] A. J. Horsewill, S. Rols, M. R. Johnson, Y. Murata, M. Murata, K. Komatsu, M. Carravetta, S. Mamone, M. H. Levitt, J. Y.-C. Chen, J. A. Johnson, X. Lei, and N. J. Turro, Phys. Rev. B **82**, 081410 (2010).
[9] S. Mamone, J. Y.-C. Chen, R. Bhattacharyya, M. H. Levitt, R. G. Lawler, A. J. Horsewill, T. Rõõm, Z. Bačić, and N. J. Turro, Coord. Chem. Rev. **255**, 938 (2011).
[10] D. Colognesi, M. Celli, L. Ulivi, M. Xu, and Z. Bačić, J. Phys. Chem. A **117**, 7314 (2013).
[11] M. Mondelo-Martell and F. Huarte-Larrañaga, J. Chem. Phys. **142**, 084304 (2015).
[12] D. E. Palin and H. M. Powell, J. Chem. Soc. , 571 (1948).
[13] T. A. Strobel, Y. Kim, G. S. Andrews, J. R. Ferrell III, C. A. Koh, A. M. Herring, and E. D. Sloan, J. Am. Chem. Soc. **130**, 14975 (2008).
[14] V. F. Rozsa and T. A. Strobel, J. Phys. Chem. Lett. **5**, 1880 (2014).
[15] A. Giannasi, M. Celli, L. Ulivi, and M. Zoppi, The Journal of Chemical Physics **129**, 084705 (2008).
[16] T. A. Strobel, E. D. Sloan, and C. A. Koh, J. Chem. Phys. **130**, 014506 (2009).
[17] T. L. Hill, J. Chem. Phys. **16**, 181 (1948).
[18] D. White and E. N. Lassettre, J. Chem. Phys. **32**, 72 (1960).
[19] R. T. Azuah, L. R. Kneller, Y. Qiu, P. W. Tregenna-Piggott, C. M. Brown, J. R. D. Copley, and R. M. Dimeo, J. Res. Natl. Inst. Stan. Technol. **114**, 341 (2009).
[20] I. F. Silvera and M. Nielsen, Phys. Rev. Lett. **37**, 1275 (1976).
[21] S. Andersson and J. Harris, Phys. Rev. Lett. **48**, 545 (1982).
[22] K. Svensson, L. Bengtsson, J. Bellman, M. Hassel, M. Persson, and S. Andersson, Phys. Rev. Lett. **83**, 124 (1999).
[23] I. Matanović, J. L. Belof, B. Space, K. Sillar, J. Sauer, J. Eckert, and Z. Bačić, J. Chem. Phys. **137**, 014701 (2012).
[24] T. Pham, K. A. Forrest, P. A. Georgiev, W. Lohstroh, D.-X. Xue, A. Hogan, M. Eddaoudi, B. Space, and J. Eckert, Chem. Commun. **50**, 14109 (2014).
[25] W. L. Queen, E. D. Bloch, C. M. Brown, M. R. Hudson, J. A. Mason, L. J. Murray, A. J. Ramirez-Cuesta, V. K. Peterson, and J. R. Long, Dalton Trans. **41**, 4180 (2012).
[26] P. C. H. Mitchell, S. F. Parker, A. J. Ramirez-Cuesta, and J. Tomkinson, *Vibrational Spectroscopy with Neutrons: with Applications in Chemistry, Biology, Materials Science and Catalysis* (World Scientific, 2005).
[27] H. Ukegawa, T. Matsuo, H. Suga, A. J. Leadbetter, R. C. Ward, and J. W. Clark, Can. J. Chem. **66**, 943 (1988).
[28] See Supplemental Materials [URL] for experimental methods and additional spectra, which includes Refs. [29-33].
[29] J. R. D. Copley and J. C. Cook, Chem. Phys. **292**, 477 (2003).
[30] S. F. Parker, F. Fernandez-Alonso, A. J. Ramirez-Cuesta, J. Tomkinson, S. Rudic, R. S. Pinna, G. Gorini, and J. F. Castañon, J. Phys.: Conf. Ser. **554**, 012003 (2014).
[31] P. A. Seeger, L. L. Daemen, and J. Z. Larese, Nucl. Instr. Meth. Phys. Res. A **604**, 719 (2009).
[32] O. Arnold, J. Bilheux, J. Borreguero, A. Buts, S. Campbell, L. Chapon, M. Doucet, N. Draper, R. F. Leal, M. Gigg, V. Lynch, A. Markvardsen, D. Mikkelson, R. Mikkelson, R. Miller, K. Palmen, P. Parker, G. Passos, T. Perring, P. Peterson, S. Ren, M. Reuter, A. Savici, J. Taylor, R. Taylor, R. Tolchenov, W. Zhou, and J. Zikovsky, Nucl. Instr. Meth. Phys. Res. A **764**, 156 (2014).
[33] C. M. Brown, Y. Liu, T. Yildirim, V. K. Peterson, and C. J. Kepert, Nanotechnology **20**, 204025 (2009).